

Article

Numerical Investigation on Injected-Fluid Recovery and Production Performance following Hydraulic Fracturing in Shale Oil Wells

Kai Liao ^{1,2,*}, Jian Zhu ², Xun Sun ³, Shicheng Zhang ² and Guangcong Ren ²¹ School of Petroleum, China University of Petroleum-Beijing at Karamay, Karamay 834000, China² School of Petroleum Engineering, China University of Petroleum (Beijing), Beijing 102299, China³ CNPC Engineering Technology R&D Company Ltd., Beijing 102206, China

* Correspondence: 2020592108@cupk.edu.cn

Abstract: Currently, volume fracturing of horizontal wells is the main technology for shale oil development. A large amount of fracturing fluid is injected into the formation, but the flowback efficiency is very low. Besides, the impact of fluid retention on productivity is not fully clear. There is still a debate about fast-back or slow-back after fracturing, and the formulation of a reasonable cleanup scheme is lacking a theoretical basis. To illustrate the injected-fluid recovery and production performance of shale oil wells, an integrated workflow involving a complex fracture model and oil-water production simulation was presented, enabling a confident history match of flowback data. Then, the impacts of pumping rate, slick water ratio, cluster spacing, stage spacing and flowback rate were quantitatively analyzed. The results show that the pumping rate is negatively correlated with injected-fluid recovery, but positively correlated with oil production. A high ratio of slick water would induce a quite complex fracture configuration, resulting in a rather low flowback efficiency. Meanwhile, the overall conductivity of the fracture networks would also be reduced, as well as the productivity, which indicates that there is an optimal ratio for hybrid fracturing fluid. Due to the fracture interference, the design of stage or cluster spacing is not the smaller the better, and needs to be combined with the actual reservoir conditions. In addition, the short-term flowback efficiency and oil production increase with the flowback rate. However, considering the damage of pressure sensitivity to long-term production, a slow-back mode should be adopted for shale oil wells. The study results may provide support for the design of a fracturing scheme and the optimization of the flowback schedule for shale oil reservoirs.

Keywords: complex fracture; flowback; productivity; numerical simulation; shale oil

Citation: Liao, K.; Zhu, J.; Sun, X.; Zhang, S.; Ren, G. Numerical Investigation on Injected-Fluid Recovery and Production Performance following Hydraulic Fracturing in Shale Oil Wells. *Processes* **2022**, *10*, 1749. <https://doi.org/10.3390/pr10091749>

Academic Editors: Linhua Pan, Yushi Zou, Jie Wang, Minghui Li, Wei Feng and Lufeng Zhang

Received: 27 July 2022

Accepted: 27 August 2022

Published: 2 September 2022

Publisher's Note: MDPI stays neutral with regard to jurisdictional claims in published maps and institutional affiliations.



Copyright: © 2022 by the authors. Licensee MDPI, Basel, Switzerland. This article is an open access article distributed under the terms and conditions of the Creative Commons Attribution (CC BY) license (<https://creativecommons.org/licenses/by/4.0/>).

1. Introduction

In recent years, the rapid development of horizontal volume fracturing technology has made shale oil another unconventional resource with huge potential value for industrial exploitation [1]. Through large-scale staged fracturing, hydraulic fractures can communicate and expand natural fractures, or induce the creation of secondary micro-fractures. In this way, complex interconnected fracture networks are formed to increase the stimulated volume, resulting in a great expansion in productivity [2]. Unlike conventional reservoirs, shale oil reservoirs use slickwater as fracturing fluids, which reduces costs and contributes to complex fractures due to their low viscosity [3]. Field data show that tens of thousands of cubic meters of fracturing fluids are injected underground, but the flowback efficiency is extremely low, leaving a large amount of water permanently trapped [4].

Current research shows that matrix imbibition and complex fracture closure are the main mechanisms of fracturing fluid retention in shale reservoirs: (1) in terms of matrix imbibition, Dutta observed the water phase imbibition process in tight cores by using real-time CT scanning technology and proposed that the low flowback efficiency was mainly

affected by rock permeability, capillary force and heterogeneity [5]. Lin carried out NMR experiments on spontaneous imbibition of shale and found that the water retention was not only controlled by capillary force but also related to chemical osmotic pressure [6]. In addition, the factors affecting the imbibition of fracturing fluid into the deep reservoir included water-rock contact area, initial water saturation and forced pressure [7,8]. (2) In terms of fracture closure, McClure M analyzed how natural fracture closure was one of the important mechanisms for fracturing fluid to be trapped underground [9]. By using analytical methods to study the dynamic flowback characteristics of a horizontal well, Ezulike and Fu found that the hydraulic fracture networks were mainly composed of unproped fractures, and the closure of these fractures would block the channels of fracturing fluid flowing to the wellbore [10,11].

Although the above studies have explained the reasons for low flowback efficiency in tight reservoirs from different perspectives, there is still a lack of clear understanding of the impact of water retention on shale oil production. Some scholars believed that the interaction between water and shale may be beneficial to increasing hydrocarbon production. Alamdari and Wang studied the impacts of reservoir wettability and natural fractures on imbibition and oil drainage and believed that the initial productivity could be improved through spontaneous imbibition of water in water-wet reservoirs or reservoirs with natural fractures [12,13]. Wang used a nano-oil displacement agent to achieve wettability reversal of oil-wet reservoir, and also observed oil drainage function by imbibition of water [14]. Dehghanpour found that hydration swelling of clay minerals can induce new micro-fractures and increase shale permeability [15]. However, other scholars held that the invasion and retention of fracturing fluid may cause damage to shale reservoirs: Bennion considered that matrix imbibition of unconventional reservoirs would increase water saturation near the fracture area, which could easily cause water lock and reduce hydrocarbon phase permeability [16]. Wang also drew a similar conclusion, noting that although the imbibition effect could improve initial production, it did not significantly increase ultimate recovery [17]. In addition, the reduction of rock permeability caused by scaling or other precipitations during fracturing fluid invasion could also affect production performance [18,19].

The flowback behaviors in shale wells have been mainly studied in three ways: laboratory experiment, analytical model and numerical simulation. The core imbibition experiment can simulate the fluid migration law during well shut-in and cleanup periods [5,6], but the experimental conditions are still quite different from the actual shale reservoir environment. Thus, it is difficult to clarify the flowback performance and its impact on productivity under real engineering conditions [20]. The analytical model based on rate transient analysis can predict flowback efficiency and well productivity [21], but there are limitations such as homogeneous reservoir description and simplified fracture characterization [22]. The numerical simulation method can take into account the impacts of imbibition and pressure-sensitivity and it is suitable for the mechanism study of oil and water migration in porous media [23]. Therefore, it is a practical method to study macroscopic flowback behaviors currently.

Still, the established numerical models have failed to simulate the flowback and production processes following hydraulic fracturing treatment accurately: (1) The injected fluid (then imbibed, retained or recovered) is directly contacted with complex fracture for a long time, so the properties of the fracture system are the key to determine the fluid distribution and migration. However, the fracture system formed by volume fracturing has strong heterogeneity in spatial distribution, geometric configuration, fracture conductivity and other properties, which is difficult to be successfully depicted [24]. Hydraulic fracture modelling is the deterministic approach to describing complex fractures. Compared with micro-seismic monitoring, numerical simulation has a lower operating cost and wider application scope. Besides, the simulated fracture system is based on geological data and treatment parameters, which leads to more practical and reliable fracture properties than that with the orthogonal or discrete fracture model [2]. Nevertheless, the integrated

simulation combining fracturing treatment and flowback process has not been reported. The former focuses on fracture mechanics, while the latter focuses on seepage behavior. (2) It is also a problem to present the initial distribution of injected fluid after fracturing. The fluid transfer between fracture and matrix has begun from the pumping process and, at the end, the water-cut near the fracture has increased to a certain extent [25]. Moreover, the loss of fracture volume (fracture closure) during fluid recovery has also been rarely reported. We believe the pumping operation and fracture closure should be related to fluid flowback and production performance. (3) Recently, studies have mainly focused on fracture complexity and its impact on water recovery and productivity. The immediate impacts of treatment parameters such as the pumping rate and the ratio of slick water have not been reported yet.

In this paper, an integrated workflow was proposed to combine complex fracture modelling and oil-water production modelling. By complete consideration of shale geological mechanics, matrix imbibition and fracture closure, the whole migration of fracturing fluid from pumping to cleanup to production was simulated, as well as the history-match of flowback data gathered from the Jimsar shale oil reservoir in China. Then, the impacts of different engineering factors on fluid recovery and oil production were quantitatively studied. This work provides a theoretical basis for understanding the distribution of fracturing fluid, flowback efficiency and its impact on productivity, with a view to guiding a reasonable flowback schedule and promoting the efficient development of shale oil.

2. Methodology

2.1. Model Description

This section describes three parts. First, the single porosity model is used to study the fluid flow for a shale oil well. Next, complex fracture modelling is adopted to generate a fracture network. Finally, a pressure-sensitivity model is proposed to characterize the fluid distribution and fracture closure. Together they form a workflow to simulate the flowback and production processes following fracturing.

2.1.1. Governing Equations of Fluid Flow

The key assumptions for building this fluid flow model are shown here. (1) The stimulated reservoir area includes two systems (matrix and complex fracture) and outside the stimulated area is assumed to be a single media (matrix). (2) Oil and water flow in the matrix and fracture systems conform to Darcy's law, and gas exsolution from oil is negligible at reservoir conditions. (3) The matrix system considers the capillary imbibition effect, which is negligible in the fracture system. (4) Fluid and rock are both slightly compressible. The matrix system considers pressure-dependent permeability, and the fracture system considers porosity and permeability. (5) The fluid flow is an isothermal process. The governing equations of oil and water flow are as follows:

$$\frac{\partial}{\partial t}(\nabla S_o \rho_o \Phi) + \nabla(\rho_o v_o) + q_o = 0 \quad (1)$$

$$\frac{\partial}{\partial t}(\nabla S_w \rho_w \Phi) + \nabla(\rho_w v_w) + q_w = 0 \quad (2)$$

Auxiliary equations:

$$S_w + S_o = 1 \quad (3)$$

$$P_c = P_o - P_w \quad (4)$$

where S_o , S_w are the saturation of oil and water phase; ρ_o , ρ_w are the density of oil and water phase; Φ is the effective porosity; v_o , v_w are the volumetric velocity of oil and water phase; q_o , q_w are the sink or source term of oil and water phase per unit reservoir volume; and P_c , P_o and P_w are the capillary pressure, the pressure of oil and water phase, respectively.

2.1.2. Complex Fracture Modelling and Gridding

The unconventional fracture model (UFM) is adopted to simulate the complex fracture configuration of fractured shale from a commercial simulator with coupled geomechanics features [26]. In UFM, the generated fracture system fully considers shale physical properties, in situ stress, natural fractures and the interaction between hydraulic fractures and natural fractures [27]. The detailed properties of the basic model are derived from a typical shale oil well with 27 fracture stages in Jimsar sag, Xinjiang, China. To skip the huge calculation problem, this work is conducted with a single or partial segment of the whole horizontal interval, and the results can be scaled back to the whole stimulated well [22]. The simulated segment scale is 460 m × 500 m × 60 m. Also, the upper and lower barriers adjacent to the oil layer are set. According to logging interpretation and related reports [25,28], input parameters of shale physical and mechanical properties are summarized in Table 1, and discrete natural fracture parameters are illustrated in Table 2. In addition, the complete parameters of the typical well are shown in Table 3, to simulate the fracture propagation during the pumping process under field conditions. Based on the generated 3D fracture properties, an auto-gridding method is used to generate the unstructured grid from UFM [29].

Table 1. Basic reservoir input parameters.

Parameters	Upper Barrier	Oil Layer	Lower Barrier
Initial reservoir pressure, MPa	37	37	37
Reservoir thickness, m	20	20	20
Matrix porosity	0.03	0.11	0.03
Matrix permeability, mD	0.001	0.01	0.001
Matrix initial water saturation	0.7	0.2	0.7
Minimum horizontal stress, MPa	54	52	56
Maximum horizontal stress, MPa	60	58	62
Young's modulus, GPa	40	27	40
Poisson's ratio	0.35	0.25	0.35
Tensile Strength, MPa	3.45	3.45	3.45

Table 2. Input parameters for natural fracture generation.

Parameters	Fracture Length, m	Fracture Orientation, °	Fracture Interval, m
Mean	20	50	6.7
Standard deviation	0	10	0

Table 3. Input well completion and schedule parameters.

Parameters	Cluster Interval, m	Slickwater Viscosity, mPa·s	Gel Water Viscosity, mPa·s	Pumping Rate, m ³ /min	Total Pumping Volume, m ³	Slickwater Ratio, %	Well Shut-In Time, d	Flowback Rate, m ³ /d (Per Stage)
Value	10	5	200	14	1300	40	56	7.0

In this grid model, the generated fracture network is divided into the hydraulic fracture (HF) and natural fracture (NF). After that, the relative permeability and capillary pressure curves for matrix (M) and fracture systems are adopted from Chen and Jurus [25,30], respectively, as shown in Figure 1. Due to the high permeability, the capillary pressure for hydraulic fracture is ignored. And the PVT parameters of fluids are according to Liao [23]. Then, with the well schedule as shown in Table 3, the fluid flow behavior in the stimulated reservoir can be described. Here the gel breaking process of fracturing fluid is assumed to be completed immediately after pumping, so the viscosities of slick and gel water are both equal to 1 mPa·s.

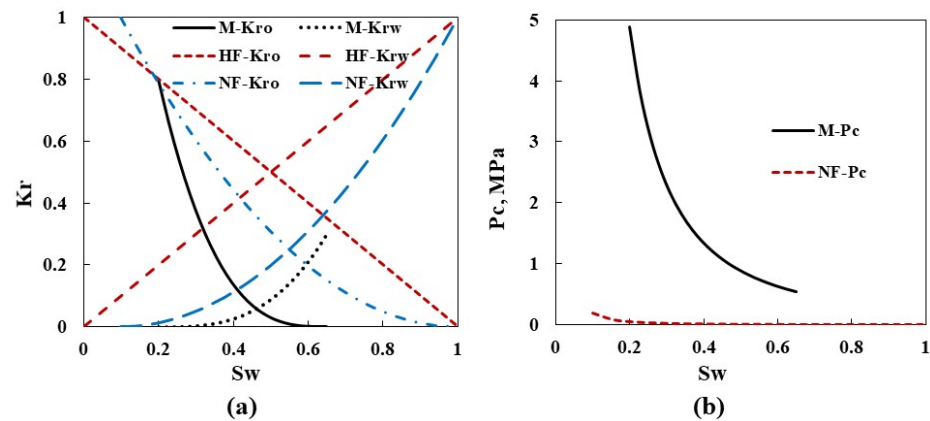


Figure 1. (a) Relative permeability curve. (b) Capillary pressure curve.

2.1.3. Pressure-Sensitivity Model Set Up

To study the fluid flow behavior, the primary task is to illustrate the distribution of reservoir pressure and saturation fields at the end of the pumping period. Therefore, oil-water production modelling needs to start with the injection of fluid. Recently, the pressure-dependent permeability of the matrix has been adopted to improve injection ability, but this method lacks rationality and overestimates the increase of shale matrix permeability [31]. Besides, it is hard to describe the key drive mechanism of fracture closure at the early period of flowback.

In this work, the decrease of matrix permeability with pressure during production is assigned according to Zhu [32]. For the pumping and flowback periods, a sensitivity model is proposed to take into account the corresponding change of porosity and permeability for fracture. This model includes two consecutive paths: (1) fracture dilation process during injection, and (2) fracture depletion process after injection. Fu indicated that fracture compressibility (C_f) could be two to three orders of magnitude higher than that of the matrix [11]. The formula Equations (5) and (6) are used to capture the significant changes in fracture porosity and permeability [23].

$$\frac{\Phi_f}{\Phi_{f0}} = e^{C_f P_{net}} \quad (5)$$

$$\frac{k_f}{k_{f0}} = 10^{m P_{net}} \quad (6)$$

where Φ_f is current fracture porosity; Φ_{f0} is initial fracture porosity; P_{net} is net pressure in fracture, MPa; k_f is current fracture permeability, mD; k_{f0} is initial fracture permeability, mD; and m is permeability changing factor, MPa^{-1} . The values of C_f and m can be obtained experimentally, or by data-fit if the experimental conditions are not available. In this paper, the C_f values of HF and NF obtained by the history-match of the pumping process are both 0.134, and the m values are 0.165 and 0.247, respectively. Also, for the flowback process, the matched C_f values are 0.016 and 0.033, and the m values are 0.048 and 0.099, respectively. The results of the pressure sensitivity model for complex fracture are presented in Figure 2.

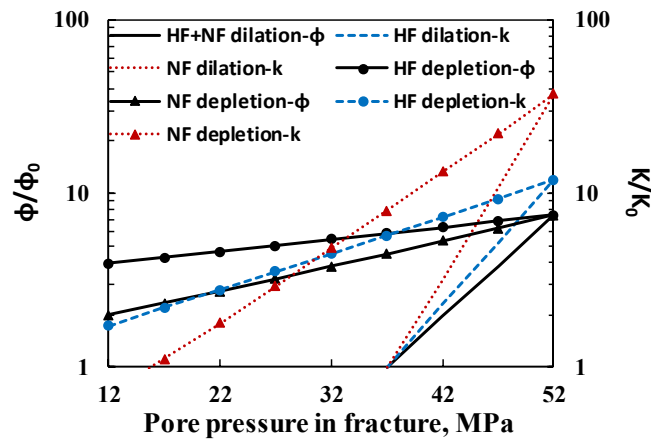


Figure 2. Pressure sensitivity curves for complex fracture from pumping to production period.

2.1.4. Integrated Workflow

As it is currently difficult to accomplish geomechanics and fluid flow mechanism within one coupled simulation at reservoir conditions, the entire workflow is divided into two steps (Figure 3). Firstly, with the input reservoir properties and treatment parameters, a complex fracture network is generated in UFM, and then finely described as an unstructured grid model. Secondly, the production modelling is conducted to forecast injected-fluid recovery and well productivity by considering capillary imbibition and pressure sensitivity in the matrix and fracture systems.

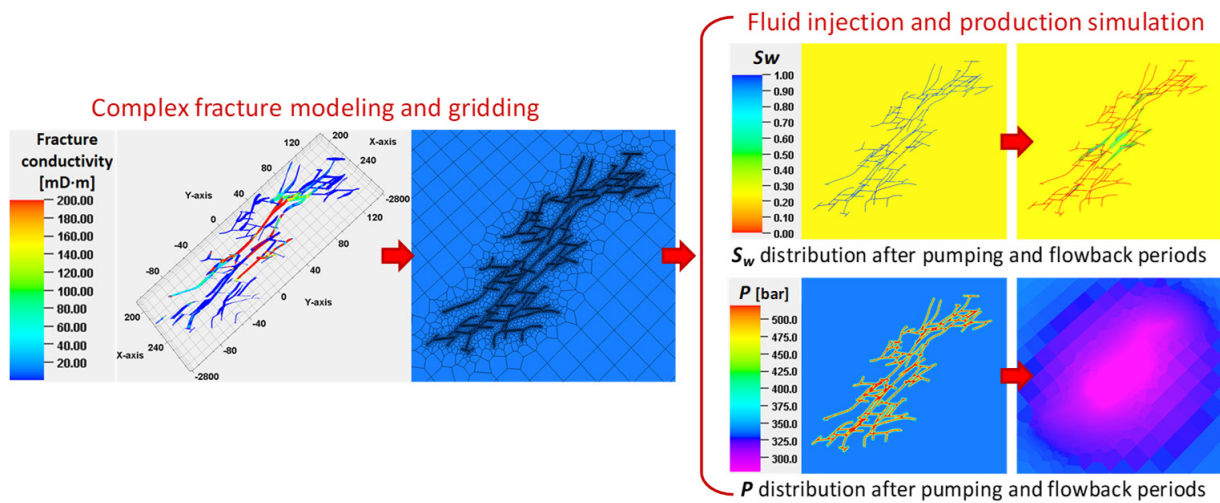


Figure 3. Numerical simulation workflow based on complex fracture modelling.

2.2. Model Validation

Due to the frequent change of choke in the early flowback stage, daily output fluctuates dramatically, which is the main challenge for quantitative validation of simulation results [22,33]. In this section, the field treatment scale (Table 3) was used to generate the complex hydraulic fracture (Figure 3). The calculated results were consistent with the micro-seismic interpretation as shown in Table 4, which verified the suitability of the proposed model to characterize complex fractures. After that, a trial-and-error method was carried out to realize the fitting between the actual and the calculated flowback performance. As the initial pressure fluctuation could easily terminate the simulation, daily liquid production data was adopted to match properly. As shown in Figure 4, the fitted results were quite acceptable, which proved the applicability and reliability of the presented workflow. Although acceptable quantitative fitting was completed, it was difficult to achieve an ideal match at the early and late stages of flowback. Since the choke size is frequently switched at the early period, higher frequency data is required to capture the

production performance, which is hard for daily output. Moreover, wellhead pressure data are generally recorded rather than reliable bottom-hole pressure, which increases uncertainty for quantitative fitting.

Table 4. Comparison of hydraulic fracture geometry.

Parameters	Fracture Half-Length, m	Fracture Bandwidth, m	Fracture Height, m
Micro-seismic interpretation of each stage	60~189	50~140	33~68
Average micro-seismic values of each stage	116.4	93.6	50.7
Calculated results	125.3	89.7	44.6

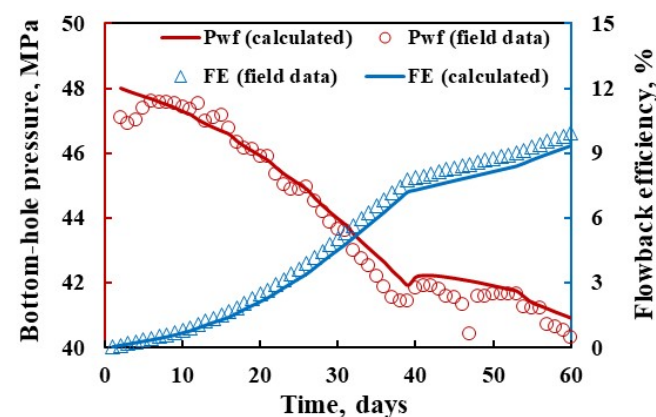


Figure 4. History-match results of bottom-hole pressure and flowback efficiency.

3. Simulation Results and Analysis

Different from conventional sandstone, due to the differences in geological features and fracturing technology, the migration of fracturing fluid in shale reservoirs is more complex. After stimulation, shale oil wells show different flowback performance from conventional ones: (1) the flowback efficiency is low and varies widely between wells; (2) there is a certain negative correlation between oil production and water recovery (flowback efficiency); (3) controlling cleanup helps increase oil production, etc. Currently, many discussions have been carried out about the impacts of shale geological factors on water imbibition and recovery, but the impacts of engineering factors on flowback behaviors are rarely studied. Therefore, this section applied the proposed models to perform a series of sensitivity analyses, which quantified the impacts of pumping rate, slick water ratio and cluster spacing. Furthermore, multi-stage fracture models were established, to investigate the impacts of stage spacing and flowback rate on water recovery and oil production.

3.1. Pumping Rate

Pumping rate is an important parameter to determine the effect of shale stimulation. Two cases of 12 and 16 m³/min were simulated and compared with the basic model (14 m³/min). The production lasts for 1 year, and the results of fracture configuration, pressure distribution, flowback efficiency and oil production are shown in Figures 5a and 6a.

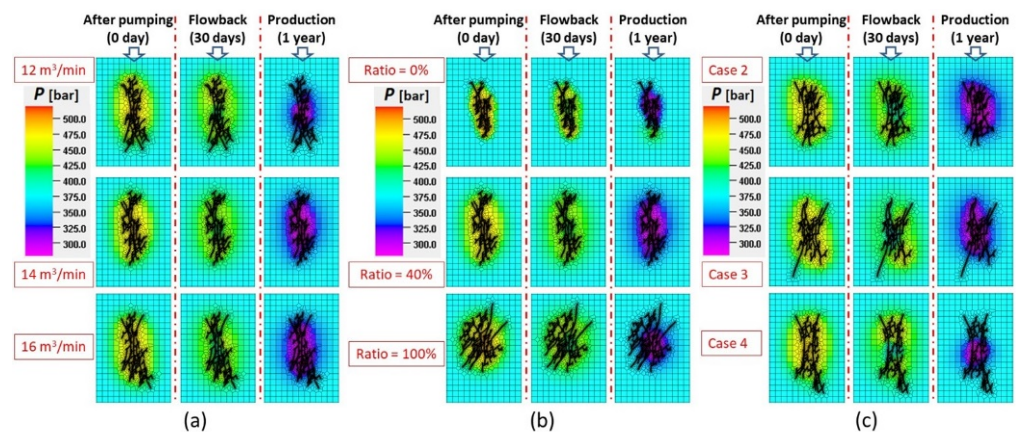


Figure 5. Variation of pressure distribution in oil layer: (a) pumping rate. (b) slick water ratio. (c) cluster spacing.

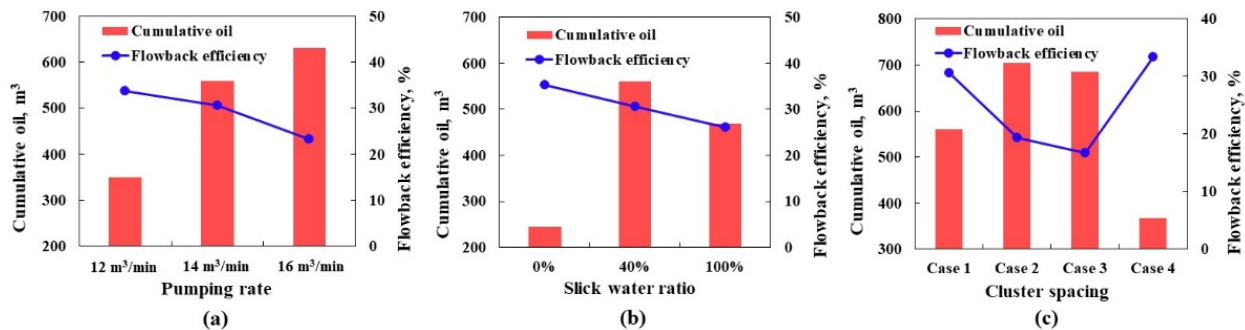


Figure 6. Cumulative oil and flowback efficiency: (a) pumping rate. (b) slick water ratio. (c) cluster spacing.

According to Figure 5a, with the increase in pumping rate, the fracture complexity in the stimulated zone will be improved, leading to a larger contact area between fracture and matrix. The imbibition is promoted further, resulting in more fracturing fluid remaining in the matrix pores near the fracture. So, as shown in Figure 6a, when the rate is 12, 14 and 16 m³/min, the flowback efficiency is 33.7%, 30.5% and 23.2%, respectively, indicating that the water recovery decreases with the increase in pumping rate.

In terms of well productivity, the cumulative oil production increases with the pumping rate, but the growth slows down. As shown in Figure 5a, although the fracture complexity at 16 m³/min is higher than that at 14 m³/min, the diffusion area of pressure drop in the two cases is almost equal after one year of production. This is because, with the same proppant quantity, the redundant natural fractures are difficult to obtain propped and gradually inactivate.

3.2. Slick Water Ratio

Currently, hybrid fracturing fluids with the alternation of gel and slick water are widely used during the stimulation treatment of shale reservoirs. Two cases of 0% (cross-linked gel alone) and 100% (slick water alone) were simulated respectively, compared with the basic model (40%). The production lasts for 1 year, and the results of fracture configuration, pressure distribution, flowback efficiency and oil production are shown in Figures 5b and 6b.

Figure 6b reports that, when the ratio is 0%, 40% and 100%, the flowback efficiency is 35.3%, 30.5% and 26.1%, respectively, indicating that the water recovery decreases with the ratio of slick water. This is due to: (1) According to Figure 5b, the fracture complexity increases significantly with the ratio of slick water, which greatly enlarges the contact area between fracture and matrix. Thus, the amount of water imbibed and retained in the

matrix increases. (2) The weak sand-carrying performance of slick water greatly reduces the fracture conductivity (F_{CD}) located in the oil layer. Figure 7 shows the F_{CD} distribution of the whole fracture system under the different ratio of slick water. Compared with the other two cases, the high permeable area near the wellbore shrinks significantly when 100% slick water is used.

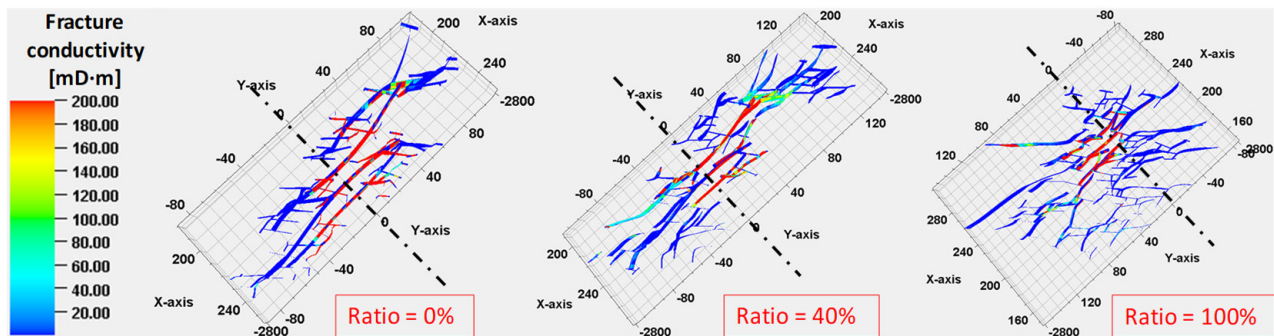


Figure 7. The F_{CD} distribution of fracture system under the different ratios of slick water (zoom scale $Z = 0.2$ times).

According to Figure 5b, when the slick water ratio is 40%, the diffusion area of pressure drop is the largest, followed by 100%, and 0% is the smallest. This trend is consistent with that of oil production in Figure 6b. Therefore, the slick water ratio may not be the higher the better, and just like the pumping rate, they all have an optimization interval. As long as the proppant quantity remains unchanged, the volume difference of the propped HF under different treatment parameters is often not very large. At this time, the reactivated NF connected with HF can play a role in increasing the drainage area. However, when the NFs are too complex, the connection between NFs is often closed due to the lack of effective support of proppant, resulting in the redundant NFs being unable to maintain long-term effective conductivity. Therefore, compared with blindly increasing the slick water ratio to form complex fractures, there may be an optimal ratio of hybrid fracturing fluids to improve the proppant carrying capacity and ensure that enough NFs are reactivated.

3.3. Cluster Spacing

The spacing or number of perforation clusters are important factors to determine the complexity of hydraulic fractures, which affect the fracturing fluid distribution and oil production performance. Within a single fracturing stage with a length of 45 m, three cases were simulated to compare with the basic case (case1, with 3 clusters and 10 m apart): (1) case 2, with 4 clusters and 12 m apart; (2) case 3, with 3 clusters and 20 m apart; (3) case 4, with 2 clusters and 30 m apart. The production lasts for 1 year, and the results of fracture configuration, pressure distribution, flowback efficiency and oil production are shown in Figures 5c and 6c.

As shown in Figure 5c, with the decrease in cluster spacing, the interference between fractures becomes more serious, resulting in more complex fractures. However, for multiple clusters, the expansion of the middle cluster is significantly worse than that of the two sides. Especially for case 2, the third cluster from the left failed to initiate. Therefore, from the fracture propagation results, the complexity of case 3 is not much different from that of case 2, and the stimulation near the well bore of case 4 is the worst. Likewise, the results of flowback efficiency and oil production are similar in case 2 and case 3, while the flowback efficiency in case 4 is the highest and the single well productivity is the lowest, as shown in Figure 6c.

The results indicate that the properly decrease of cluster spacing is conducive to increasing the contact area between fractures and matrix. But when the cluster spacing is less than 20 m, the interference may affect the stimulation effect. By comparing case 1 and

case 3, it can also be realized that the decrease in cluster spacing is not conducive to oil production when the number of perforating clusters is the same.

3.4. Stage Spacing

Stage spacing also affects the flowback and production performance in shale oil reservoirs. Within a horizontal interval length of 225 m, three cases were simulated: (1) case 1, with 5 stages and 45 m apart; (2) case 2, with 4 stages and 56 m apart; and (3) case 3, with 3 stages and 75 m apart. Figure 8 shows the results of complex fracture propagation under different stage spacing. It can be seen that: (1) In all cases, the sum of single stage stimulation width is wider than the corresponding whole well stimulation width, indicating that the fracturing area of each stage has a certain degree of overlap. (2) With the decrease of spacing, the degree of overlap becomes higher. Moreover, compared with case 2, the overall fracture complexity of case 1 is relatively close, and only the local area near the well bore is more fully stimulated.

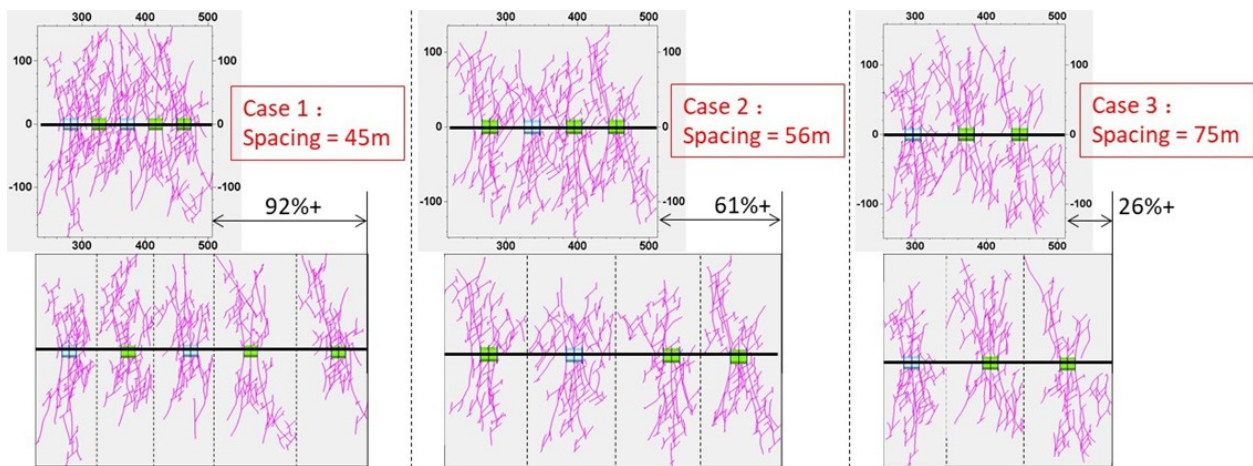


Figure 8. Complex fracture configuration under different stage spacing (global scale vs. individual scale).

Figure 9a shows that: (1) the load-recovery efficiencies of the three cases are 25.8%, 28.6% and 32.2%, respectively, which increase with the stage spacing. (2) Conversely, the oil production increases with the spacing narrowing, but the growth slows down. Furthermore, the average cumulative oil production of each individual stage is 447.7 m³, 509.8 m³ and 519 m³ for the three cases, indicating that the production contribution of a single stage is positively correlated with its spacing. This is because, although the fracture complexity increases obviously with the reduction of stage spacing, the stimulation and drainage area of the individual stage is narrowed down accordingly.

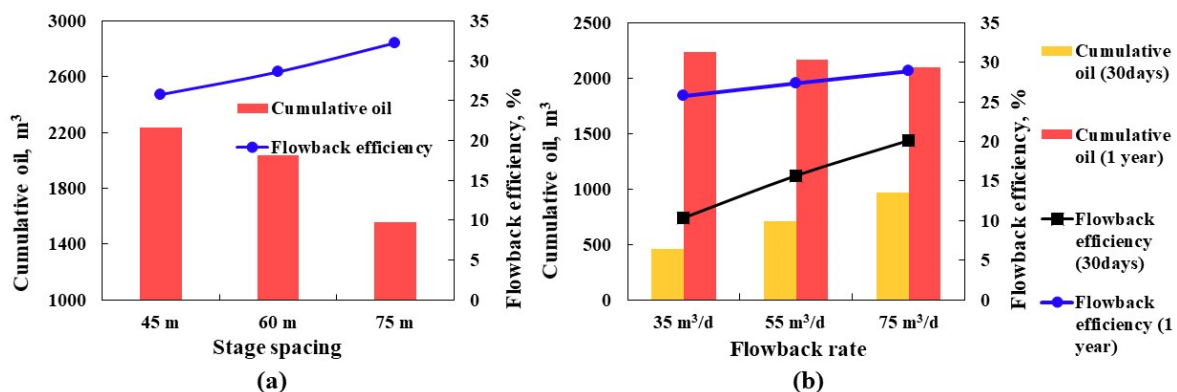


Figure 9. Cumulative oil and flowback efficiency profiles: (a) stage spacing. (b) flowback rate.

As shown in Figure 10a, the diffusion area of pressure drop in case 3 is the smallest, while those in the other two cases are relatively close after one year of production. It follows that for multi-stage fracturing treatment, reducing the stage spacing can improve productivity to some extent. However, if the total length of horizontal interval remains unchanged, it also means an increase in the number of fracturing stages, resulting in a rising fracturing operation cost and tool cost. Therefore, the design of stage spacing is not the smaller the better, and needs to be combined with the actual reservoir conditions.

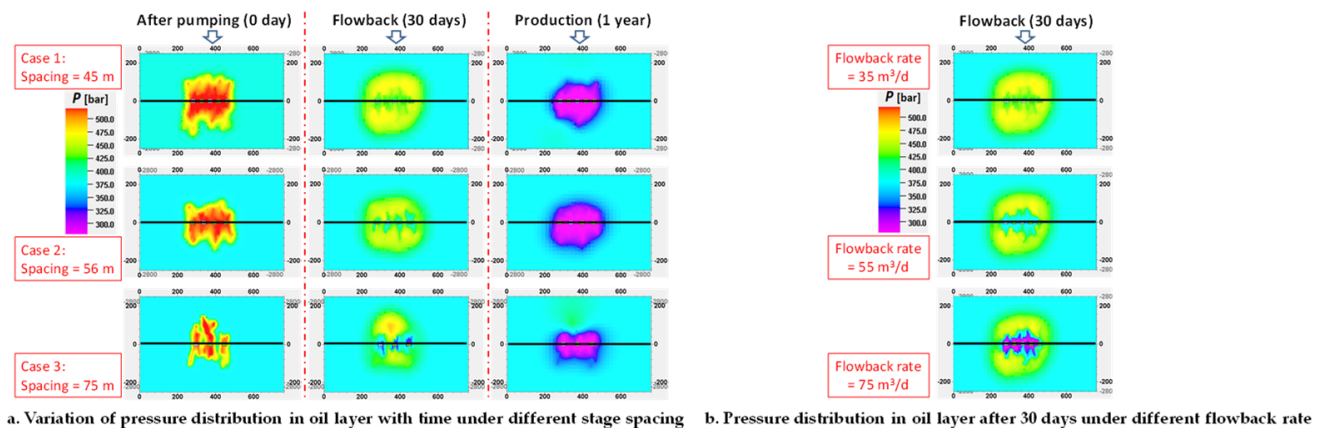


Figure 10. Variation of pressure distribution in oil layer: (a). stage spacing. (b). flowback rate.

3.5. Flowback Rate

The fracturing fluid recovery is controlled by the adjustment of choke size. Slow-back with a small choke size may delay the payback point, while fast-back with a large choke size may damage the fracture conductivity or matrix permeability [34]. To demonstrate the impact of choke size on well performance, three cases with different flowback rates of 35, 55 and 75 m³/d were simulated.

Figure 9b shows that: (1) After 1 month of production, both the water recovery and cumulative oil production increase almost linearly with the flowback rate. (2) After 1 year of production, the water recovery is still positively correlated, while the oil production is negatively correlated with the flowback rate. This reversal is due to the fact that the fast-back will force fracture closure to accelerate, and the flowback fluid is mainly water, which has not yet entered the deep matrix. Thus, the pressure depletion will be excessively consumed in water recovery, which is not conducive to later oil drainage. Additionally, according to Figure 10b, the pressure depletion near the well bore increases with the flowback rate, resulting in gradually significant damage to fracture conductivity and matrix permeability. Therefore, it is suggested to adopt a slow-back mode with a small choke size when designing the cleanup schedule of shale oil fractured wells.

4. Conclusions

Based on the typical data of a shale oil fractured well, a series of numerical models coupling complex fracture propagation and flowback simulation were established. The history match of the basic model verifies the adaptability of the proposed workflow. Accordingly, the distributions of pore pressure and fracturing fluid underground during the pumping, cleanup and production periods are accurately described, which provides a reliable basis for the study of oil-water production performance.

Pumping rate, slick water ratio and cluster spacing all affect the flowback efficiency of shale fractured wells, which is mainly reflected in the complex fracture configuration differences formed under these engineering factors, thus changing the distribution law of fracturing fluid in the formation. With the increase in pumping rate, water recovery decreases and oil production increases. The flowback efficiency increases with the increase of the slick water ratio, but from the perspective of productivity there is an optimal ratio

for hybrid fracturing fluid. Significant fracture interference may occur if the perforation clusters are too dense, so the cluster spacing is not the smaller the better.

With the decrease of stage spacing along the horizontal well, the fracture merging between adjacent fracturing stages becomes more significant. Thus, the fracture complexity increases and the water recovery decreases accordingly. Single well productivity increases with the decrease of stage spacing, but the increase gradually decreases. When the total length of the horizontal well remains the same, considering the cost of fracturing operations and tool use, the interval design is not the smaller the better, but needs to be combined with the actual reservoir conditions.

For the schedule of flowback in shale fractured wells, the slow-back mode should be adopted. This is because fast-back will cause the supplementary formation pressure during fracturing to be excessively consumed in the subsequent water recovery. It may also cause significant pressure-sensitive damage in the near-well area, which is not conducive to long-term production.

Author Contributions: Methodology, K.L.; validation, K.L., J.Z. and X.S.; writing—original draft preparation, K.L. and J.Z.; writing—review and editing, S.Z.; language check, G.R. All authors have read and agreed to the published version of the manuscript.

Funding: This research was funded by Research Foundation of China University of Petroleum-Beijing at Karamay (No. XQZX20220003); Natural Science Foundation of Xinjiang Uygur Autonomous Region (No. 2022D01B79).

Institutional Review Board Statement: Not applicable.

Informed Consent Statement: Not applicable.

Data Availability Statement: Not applicable.

Acknowledgments: This work was jointly supported by the Research Foundation of China University of Petroleum-Beijing at Karamay and the Natural Science Foundation of Xinjiang Uygur Autonomous Region.

Conflicts of Interest: The authors declare no conflict of interest.

References

1. Zhou, L.; Zhao, X.; Chai, G.; Jiang, W.; Pu, X.; Wang, X.; Han, W.; Guan, Q.; Feng, J.; Liu, X. Key exploration & development technologies and engineering practice of continental shale oil: A case study of Member 2 of Paleogene Kongdian Formation in Cangdong Sag, Bohai Bay Basin, East China. *Pet. Explor. Dev.* **2020**, *47*, 1059–1066.
2. Pu, C.; Zheng, H.; Yang, Z.; Gao, Z. Research status and development trend of the formation mechanism of complex fractures by staged volume fracturing in horizontal wells. *Acta Pet. Sin.* **2020**, *41*, 1734–1743.
3. Palisch, T.T.; Vincent, M.C.; Handren, P.J. Slickwater Fracturing: Food for Thought. *SPE Prod. Oper.* **2010**, *25*, 324–344. [[CrossRef](#)]
4. Gao, Z.; Qu, X.; Huang, T.; Xue, T.; Cao, P. Stress sensitivity analysis and optimization of horizontal well flowback system for shale oil reservoir in Ordos Basin. *Nat. Gas Geosci.* **2021**, *32*, 1867–1873.
5. Dutta, R.; Lee, C.H.; Odumabo, S.; Ye, P. Experimental Investigation of Fracturing-Fluid Migration Caused by Spontaneous Imbibition in Fractured Low-Permeability Sands. *SPE Reserv. Eval. Eng.* **2014**, *17*, 74–81. [[CrossRef](#)]
6. Hun, L.; Shicheng, Z.; Fei, W.; Ziqing, P.; Jianye, M.; Tong, Z.; Zongxiao, R. Experimental Investigation on Imbibition-front Progression in Shale Based on Nuclear Magnetic Resonance. *Energy Fuels* **2016**, *30*, 9097–9105. [[CrossRef](#)]
7. Xu, G.; Shi, Y.; Jiang, Y.; Jia, C.; Gao, Y.; Han, X.; Zeng, X. Characteristics and Influencing Factors for Forced Imbibition in Tight Sandstone Based on Low-Field Nuclear Magnetic Resonance Measurements. *Energy Fuels* **2018**, *32*, 8230–8240. [[CrossRef](#)]
8. Xu, G.; Jiang, Y.; Shi, Y.; Han, Y.; Wang, M.; Zeng, X. Experimental Investigation of Fracturing Fluid Flowback and Retention under Forced Imbibition in Fossil Hydrogen Energy Development of Tight Oil Based on Nuclear Magnetic Resonance. *Int. J. Hydrogen Energy* **2020**, *45*, 13256–13271. [[CrossRef](#)]
9. McClure, M. The potential effect of network complexity on recovery of injected fluid following hydraulic fracturing. In Proceedings of the SPE Unconventional Resources Conference, The Woodlands, TX, USA, 1–3 April 2014.
10. Ezulike, D.O.; Dehghanpour, H.; Virues, C.J.; Hawkes, R.V.; Jones, R.S. Flowback Fracture Closure: A Key Factor for Estimating Effective Pore Volume. *SPE Reserv. Eval. Eng.* **2016**, *19*, 567–582. [[CrossRef](#)]
11. Fu, Y.; Dehghanpour, H.; Ezulike, D.O.; Jones, R.S.J. Estimating effective fracture pore volume from flowback data and evaluating its relationship to design parameters of multistage-fracture completion. *SPE Prod. Oper.* **2017**, *32*, 423–439. [[CrossRef](#)]

12. Alamdari, B.B.; Kiani, M.; Kazemi, H. *Experimental and Numerical Simulation of Surfactant-Assisted Oil Recovery in Tight Fractured Carbonate Reservoir Cores*; SPE Improved Oil Recovery Symposium: Tulsa, OK, USA, 2012.
13. Jing, W.; Huiqing, L.; Genbao, Q.; Yongcan, P.; Yang, G. Investigations on spontaneous imbibition and the influencing factors in tight oil reservoirs. *Fuel* **2019**, *236*, 755–768. [[CrossRef](#)]
14. Wang, C.; Cui, W.; Zhang, H.; Qiu, X.; Liu, Y. High efficient imbibition fracturing for tight oil reservoir. In Proceedings of the SPE Trinidad and Tobago Section Energy Resources Conference, Port of Spain, Trinidad and Tobago, 25–26 June 2018.
15. Dehghanpour, H.; Lan, Q.; Saeed, Y.; Fei, H.; Qi, Z. Spontaneous Imbibition of Brine and Oil in Gas Shales: Effect of Water Adsorption and Resulting Microfractures. *Energy Fuels* **2013**, *27*, 3039–3049. [[CrossRef](#)]
16. Bennion, D.B.; Thomas, F.B.; Bietz, R.F.; Bennion, D.W. Water and hydrocarbon phase trapping in porous media—diagnosis, prevention and treatment. *J. Can. Pet. Technol.* **1996**, *35*, 29–36. [[CrossRef](#)]
17. Wang, M.; Leung, J.Y. Numerical investigation of fluid-loss mechanisms during hydraulic fracturing flow-back operations in tight reservoirs. *J. Pet. Sci. Eng.* **2015**, *133*, 85–102. [[CrossRef](#)]
18. Khormali, A.; Petrakov, D.G.; Farmanzade, A.R. Prediction and Inhibition of Inorganic Salt Formation under Static and Dynamic Conditions—Effect of Pressure, Temperature, and Mixing Ratio. *Int. J. Technol.* **2016**, *7*, 943–951. [[CrossRef](#)]
19. Khormali, A.; Bahlakeh, G.; Struchkov, I.; Kazemzadeh, Y. Increasing inhibition performance of simultaneous precipitation of calcium and strontium sulfate scales using a new inhibitor—Laboratory and field application. *J. Pet. Sci. Eng.* **2021**, *202*, 108589. [[CrossRef](#)]
20. Zhang, T.; Li, X.; Yang, L. Effects of shut-in timing on flowback rate and productivity of shale gas wells. *Nat. Gas Ind.* **2017**, *37*, 48–60.
21. Zhang, Z.; Clarkson, C.; Williams-Kovacs, J.D.; Yuan, B.; Ghanizadeh, A. Rigorous Estimation of the Initial Conditions of Flowback Using a Coupled Hydraulic-Fracture/Dynamic-Drainage-Area Leakoff Model Constrained by Laboratory Geomechanical Data. *SPE J.* **2020**, *25*, 3051–3078. [[CrossRef](#)]
22. Zhang, T.; Li, X.; Li, J.; Feng, D.; Li, P.; Zhang, Z.; Chen, Y.; Wang, S. Numerical investigation of the well shut-in and fracture uncertainty on fluid-loss and production performance in gas-shale reservoirs. *J. Nat. Gas Sci. Eng.* **2017**, *46*, 421–435. [[CrossRef](#)]
23. Liao, K.; Zhang, S.; Ma, X.; Zou, Y. Numerical Investigation of Fracture Compressibility and Uncertainty on Water-Loss and Production Performance in Tight Oil Reservoirs. *Energies* **2019**, *12*, 1189. [[CrossRef](#)]
24. Li, L.; Jiang, H.; Li, J.; Wu, K.; Meng, F.; Chen, Z. Modeling tracer flowback in tight oil reservoirs with complex fracture networks. *J. Pet. Sci. Eng.* **2017**, *157*, 1007–1020. [[CrossRef](#)]
25. Chen, X.; Liao, K.; Lv, Z.; Zhu, J.; Wang, J.; Li, Y.; Wang, F. Numerical Simulation Study on Optimal Shut-in Time in Jimsar Shale Oil Reservoir. *Front. Energy Res.* **2022**, *10*, 849064. [[CrossRef](#)]
26. Weng, X.; Kresse, O.; Chuprakov, D.; Cohen, C.E.; Prioul, R.; Ganguly, U. Applying complex fracture model and integrated workflow in unconventional reservoirs. *J. Pet. Sci. Eng.* **2014**, *124*, 468–483. [[CrossRef](#)]
27. Yan, X.; Mou, J.; Tang, C.; Xin, H.; Zhang, S.; Ma, X.; Duan, G. Numerical Investigation of Major Impact Factors Influencing Fracture-Driven Interactions in Tight Oil Reservoirs: A Case Study of Mahu Sug, Xinjiang, China. *Energies* **2021**, *14*, 4881. [[CrossRef](#)]
28. Baocheng, W.U.; Jianmin, L.I.; Yuanyue, W.U.; Le, H.; Tingfeng, Z.; Yushi, Z. Development practices of geology-engineering integration on upper sweet spots of Lucaogou Formation shale oil in Jimsar sag, Junggar Basin. *China Pet. Explor.* **2019**, *24*, 679–690.
29. Cipolla, C.L.; Fitzpatrick, T.; Williams, M.J.; Ganguly, U.K. Seismic-to-simulation for unconventional reservoir development. In Proceedings of the SPE Reservoir Characterisation and Simulation Conference and Exhibition, Abu Dhabi, United Arab Emirates, 9–11 October 2011.
30. Jurus, W.J.; Whitson, C.H.; Golan, M. Modeling water flow in hydraulically-fractured shale wells. In Proceedings of the SPE Annual Technical Conference and Exhibition, New Orleans, LA, USA, 30 September–2 October 2013.
31. Ehlig-Economides, C.A.; Ahmed, I.; Apiwathanasorn, S.; Lightner, J.; Song, B.; Vera, F.; Xue, H.; Zhang, Y. Stimulated shale volume characterization: Multiwell case Study from the Horn River shale: II. Flow perspective. In Proceedings of the SPE Annual Technical Conference and Exhibition, San Antonio, TX, USA, 8–10 October 2012.
32. Zhu, W.; Ma, D.; Zhu, H.; An, L.; Li, B. Stress sensitivity of shale gas reservoir and influence on productivity. *Nat. Gas Geosci.* **2016**, *27*, 892–897.
33. Wang, M.; Leung, J.Y. Numerical investigation of coupling multiphase flow and geomechanical effects on water loss during hydraulic-fracturing flowback operation. *SPE Reserv. Eval. Eng.* **2016**, *19*, 520–537. [[CrossRef](#)]
34. Fu, Y.; Dehghanpour, H.; Motealleh, S.; Lopez, C.M.; Hawkes, R. Evaluating fracture volume loss during flowback and its relationship to choke size: Fastback vs. slowback. *SPE Prod. Oper.* **2019**, *34*, 615–624. [[CrossRef](#)]